International Journal of Engineering & Technology, 7 (4.14) (2018) 401-405

International Journal of Engineering & Technology

Website: www.sciencepubco.com/index.php/IJET

Research paper



Surface Defect Detection using Novel Histogram Distance-based Multiple Template Anomalies Detection Algorithm

Ze-Hao Wong[1], C.M. Thong[1], W.M. Edmund Loh[2], C.J. Wong[2]*

[1]ViTrox Campus 2.0, 746, Persiaran Cassia Selatan 3, Batu Kawan Industrial Park, 14110 Bandar Cassia, Penang, Malaysia.
[2]School of Physics, Universiti Sains Malaysia, 11800 USM, Penang, Malaysia.
**Corresponding author E-mail: wongcj@usm.my*

Abstract

Surface defects in manufacturing are top challenges in various manufacturing field including LED manufacturing, die manufacturing and printing industry. Quality control through automated surface defect detection has been an emphasis to speed up the production without jeopardizing the quality of the product. However, complexity and flexibility in product design, specification and dataset availability posted challenges in existing referential-based algorithm. Golden template-based algorithms are sensitive to misalignment and product variations. Deep learning and its variant can be used as non-linear filter to segment anomalies area. However, deep learning requires huge labelled database and consume long learning time. Similarly, maximum likelihood-based algorithms require large database for learning. This research proposes a novel histogram distance based multiple templates anomalies detection (MTAD) algorithm to segment surface defect. Histogram distance based on kernel-wise histograms stacked across illumination normalized database of similar size can describe the degree of anomaly intuitively across the image. Then, surface defect can be justified intuitively according to anomaly heat map generated. The algorithm is tested against industrial samples and it can handle texture and design variation existed in the product while catching anomaly in real time. This research suggests future studies on extending dimensionality of the histogram. Suggested algorithm has wide range of application other than surface defect detection. For examples, video motion detection, decolorization detection on industrial lighting.

Keywords: *Histogram distance; Multiple templates; Referential method; Surface Defect Detection*

1. Introduction

Surface defect detection is a qualitative inspection which involves detecting fault which are not quantifiable. This includes extra parts, foreign materials, contamination and cracks [1]. Machine vision techniques are widely used toward surface detection problems [2]. Many algorithms have been explored and proposed over the last decades, but they share one thing in common: detecting anomalies which is different from their background [3] or their intended design. Intension to replace human operator in manual vision inspection (MVI) has motivated continuous active research and application in industrial [4], especially as industry is evolving towards industry 4.0.

2. Related Works

Surface defect detection algorithms can be categorized into non-referential, referential and hybrid [5], [6]. Non-referential approaches do not use any referential image for learning or comparison [7], [8]. On the other hand, Referential approach uses either a golden reference or a set of references for image or feature comparison to extract surface defect.

However, reference used for comparison and defect extraction is not restricted to image only. Ibrahim et al transform both reference and sample image using wavelet transform, containing horizontal and vertical details of the images in different level, for anomalies extraction [9]. Normalized cross-correlation based algorithm was proposed, to detect anomalies based on sub-region similarity of pixels [10]. However, alignment accuracy is crucial to its detection accuracy. Q-Q plot based pattern matching algorithm as a more superior method to NCC based algorithm is proposed [11]. It uses quantile to quantile plot of a sub-regional pixel as feature comparison. A novel shift-tolerant dissimilarity measure approach is proposed less than a decade ago. It uses optical flow field to indicate degree of difference between a reference and a sample [12]. This approach can outperform conventional template matching method. Gaidhane et al proposed an efficient similarity approach for reference-based surface defect detection. It's similarity measure is based on the rank of symmetric matrix computed using companion matrices between a reference and a sample [13]. Due to its efficiency for computation, it is found to be faster than optical flow method proposed by Tsai. However, the degree of difference in either method do not have an intuitive link to the physical properties of the image. Son proposed Fisher information distance of local Gaussian distribution between reference and sample as a defect measure for surface defect detection on OLED product [6]. Moreover, Kong et al proposed a complete framework from automatic template selection from a set of references, robust registration and surface defect segmentation based on edge point [14]. The framework itself is a generalization of a system design which is adoptable in many cases. However, involvement of randomness in optimization step might render slightly different result in regis-

Copyright © 2018 Authors. This is an open access article distributed under the Creative Commons Attribution License, which permits unrestricted use, distribution, and reproduction in any medium, provided the original work is properly cited.

tration and hence surface defect detection. Ren et al proposed the use of pretrained deep neural network classifier (Decaf) which build based on feature of image patches as surface defect detection method [15]. Defective region is computed pixel by pixel through convolving classifier with input image. They claimed that learning involved very little samples where good samples can be gotten within the same input. However, real time application is still in progress of research.

3. Proposed Work

We propose a novel anomaly detection algorithm using multiple templates or references. Like most reference-based surface defect algorithm, the whole process involved learning and inspection. Unlike methods which need automatic template selection [14] or golden template [8], proposed will generate a consolidated reference table of histogram distances based on grey value distribution of local region. For this reason, the database size remains constant when more reference images are added in. This make the algorithm scalable to any number of reference image. We use automated unsupervised clustering for grey-scale distribution. For each cluster, a histogram distance model is computed based on special case of L_2 norm. Probabilistic combination of each histogram distance model will form a distance reference table for each pixel location. The learning process ended with the completion of reference table. Inspection of surface defect involves generating heat map by referring its gray value to the reference table at its location. Generated heat map retains its physical properties of grey value. This gave intuitiveness in understanding when analyzing heat map and deciding the decision boundary for defect. Following subsections describe details in each process.

3.1. Simple image registration and pre-processing

Similar approach of image registration and pre-processing are applied before learning algorithm and inspection algorithm. Differences in image registration and preprocessing might cause small undesired variation in output. Small difference might be insignificant in other applications, strict repeatability and reproducibility in industrial inspection system cannot tolerance addition variations from algorithm. In our study, Fast Normalized Cross-Correlation (FNCC) is used as image registration algorithm for both learning and inspection. FNCC algorithm is widely used and well-documented [16]. Then, input image is filtered using Gaussian filter for minor noise reduction.

3.2. 1D Histogram Generation and Clustering

A set of pre-processed and pre-registered reference images with same size are used to generate pixel-wise 1-dimensional histogram. For each pixel, a kernel size of k_m x k_n centered at the pixel is used to fill histogram for that location across all reference images. For a reference image of size L_t = W_t x H_t , there will be L_t or less 1D histogram. For each histogram, a novel DBSCAN parameter estimation using trimmed statistical properties is proposed to find unsupervised clustering parameter adaptively. DBSCAN stands for density based spatial clustering of application with noise, defines each data points into core points, density-reachable points and outliers based on radius, *r* and number of minimum points, *minPts*.

By excluding all classes below a defined frequency, τ and reordering remaining classes, a trimmed histogram is yielded. A trimmed histogram is invariant to clusters' gap and resistant to variation in total frequency. The mean and standard deviation of a trimmed histogram is defined in Equation (1) and (2) respectively.

$$\mu_{trimmed} = \sum_{i=0}^{N} \{\pi_i \cdot h_i[h_i > \tau]\} \Big/ \eta \tag{1}$$

$$\sigma_{trimmed} = \sqrt{\frac{SS_t}{\eta} - \mu_{trimmed}^2} \tag{2}$$

where

$$\pi_i = \sum_{k=0}^{i} [h_k > \tau] \tag{3}$$

$$\eta = \sum_{i=0}^{N} h_i[h_i > \tau] \tag{4}$$

We propose that DBSCAN's parameters can be estimated using trimmed histogram's mean, $\mu_{trimmed}$, standard deviation, $\sigma_{trimmed}$ and expected frequency, $\bar{f}$. An expected frequency can be expressed by dividing the total frequency, η and trimmed histogram length, π_N . By considering the density function, $\bar{f} = {minPts}/{L}$, where L is the size of a kernel, DBSCAN's kernel size, $minPts$ and L can be estimated using Equation (6) and (6).

$$minPts = \frac{\eta \cdot L}{\pi_N} \tag{5}$$

$$L = 2 \cdot \left(\left\lfloor n \cdot \sigma_{trimmed} + \frac{1}{2} \right\rfloor \sqrt{1} \right) + 1 \tag{6}$$

where L = 3,4,5,6, …

By using estimated parameters, 1D DBSCAN is carried uniquely for each histogram at their location, retaining their histogram properties. This step can be understood as automated grayscale clustering for each pixel according to the set of reference image. Clustering allows variations of feature in term of grey-scale in reference image.

3.3. Special case of L-2 Norm Histogram Distance

For each clustered histogram, a histogram distance function is estimated for cluster independently. A histogram distance function is used in this study as dissimilarity measure to describe the degree of anomalies for each pixel. Distance measure is defined as Equation (7).

$$D_i = \sqrt{i^2 - 2i\mu + (\mu^2 + \sigma^2)} \tag{7}$$

The equation above is a special case of L2 Norm between two 1D histograms where one of the histograms has frequency of 1, expressed in term of basic statistical: mean, μ and standard deviation, σ of a cluster.

3.4. Probabilistic combination of histogram distance

As there might be multiple set of histogram distance tables within the same location, a combination of histogram distance is proposed based on Gaussian probabilistic function. For each cluster existed within a histogram, a weight based on Gaussian probabilistic function using mean and standard deviation for each cluster. Weight for each cluster and each histogram bin denoted as $W_c(i)$ can be expressed as Equation ((8) below. Distance function for each location is a linear combination of product of cluster's weight and distance as expressed in Equation (9).

$$W_c(i) = e^{\frac{-(i-\mu_c)^2}{2\sigma_c^2}} \tag{8}$$

$$D(i) = \frac{\sum_c W_c(i) \cdot D_c(i)}{\sum_c W_c(i)} \quad (9)$$

As $W_c(i)$ decay to almost non-existence after few σ_c away from μ_c, Gaussian probabilistic combination of histogram distances of various clusters retains the original histogram distance function at the center of their respective cluster and connects histogram distances at the boundaries between clusters smoothly.

3.5. Surface Defect Detection

During learning, a reference table of histogram distances is generated according to the description given in pervious subsections. A summary of algorithm is summarized as following.

Algorithm 1: Reference Table of Histogram distances computation from multiple templates

Data:
- T_0: First good reference image
- $\hat{I}$: An array of N reference images denoted as $I_i, i \in \{0,1,2,\cdots,N\}$
- W: Width of reference images
- H: Height of reference images

Result:
- $\hat{R}$: Reference table of histogram distances

Begin
- **For** $i = 0$ to N
  - Register I_i with T_0 using FNCC.
  - Denoise I_i using Gaussian filter.
  - **For** $y = 0$ to H
    - **For** $x = 0$ to W
      - Fill 1-D Histogram at (x,y) using kernel with size $k_m \times k_n$.
    - **End**
  - **End**
- **End**
- **For** $y = 0$ to H
  - **For** $x = 0$ to W
    - Estimate minPts and L using Equation (5) and (6).
    - Cluster histogram at (x,y) using DBSCAN with estimated parameter.
    - Compute distance function using Equation (9).
    - Fill computed distance function into $\hat{R}$.
  - **End**
- **End**

End

Upon the completion of reference table for histogram distances using **Algorithm 1**, surface defect heat map of a pre-registered sample image can be generated pixel-wise easily. The degree of anomaly for each pixel in input image can be obtain using precomputed distance function in the reference table. After surface heat map is generated, defective region in the image can be segmented easily. In this study, hysteresis thresholding with 50% lower on second threshold is used for defect binarization. Selection of threshold is intuitive in our proposed as the original unit for grey-value is remained. Threshold selection process can be thought as defining how brighter or darker is the defect from its intended design. The process can be summarized as **Algorithm 2** shown below.

Algorithm 2: Defect detection using reference table of histogram distances

Data:
- $\hat{R}$: Reference table of histogram distances
- T_0: First good reference image
- S: Input sample image for inspection
- W: Width of registered images
- H: Height of registered images
- M: Surface defect heat map
- τ: Degree of anomaly threshold

Result:
- $\hat{R}$: Reference table of histogram distances

Begin
- Register S with T_0 using FNCC.
- Denoise S using Gaussian filter.
- **For** $y = 0$ to H
  - **For** $x = 0$ to W
    - Get grey value of processed S at (x,y), g.
    - Get degree of anomaly from $\hat{R}$ at (x,y,g).
    - Fill M.
  - **End**
- **End**
- Do hysteresis thresholding on M with τ at 50%.

End

4. Experiment Results

We conduct defect detection analysis on industrial samples using proposed algorithm. Images of an unpopulated location from PCB unit are captured under controlled environment. **Fig. 1** is an example of the unpopulated location. An unpopulated area of a PCB board is meant to free from any foreign material. Examining the samples, we are using, unremoved stickers and solder splash are common foreign material contaminated the unpopulated area. A total of 60 images from 20 PCBs are picked. Each image has size of 400×227. There are total 51 images contains foreign material, mostly unremoved stickers. Remaining 9 images are free from foreign material. They have minor but noticeable textural difference across the samples. Moreover, samples show variation on pin-through holes' location and printed circuits. By using image difference algorithms, such variations will result in false calls. **Fig. 2** is a comparison of defect segmented using image difference algorithms with suggested algorithm. There are false calls around pin through hole areas for Image difference algorithm with auto-thresholding. When we aimed to avoid calls around pin through hole areas, it reduces defect detection capability at the same time. However, there is none using proposed algorithm.

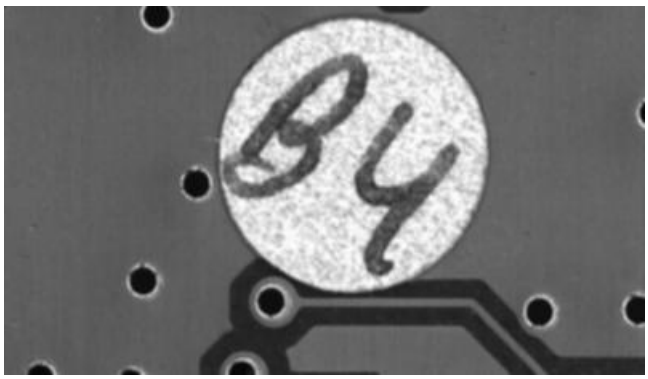

Fig. 1: Unpopulated location on industrial PCB contaminated with foreign material: unremoved stickers.

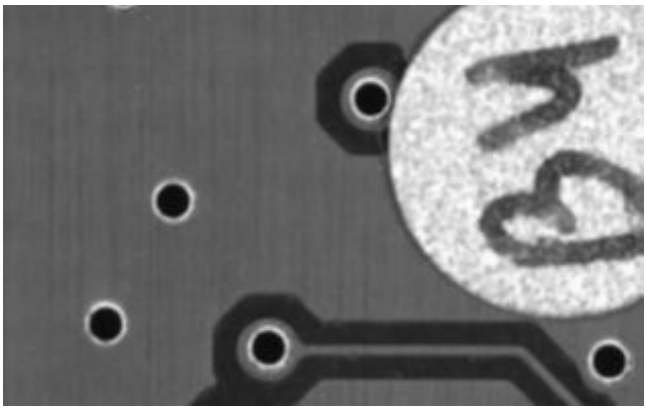

(a)

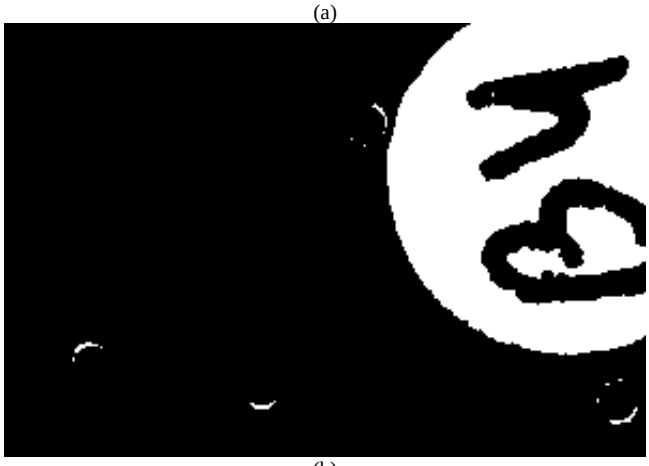

(b)

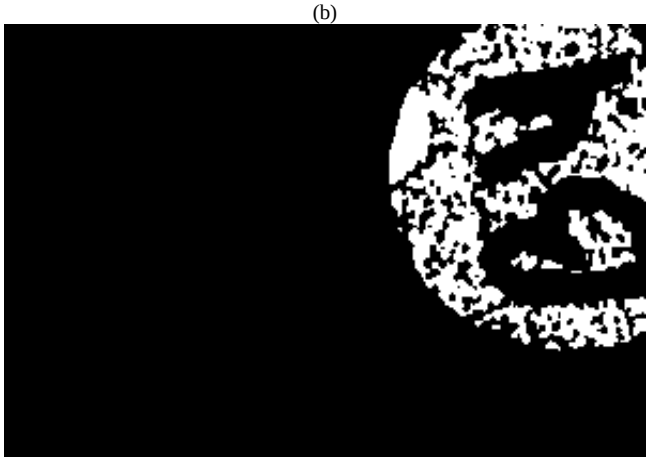

(c)

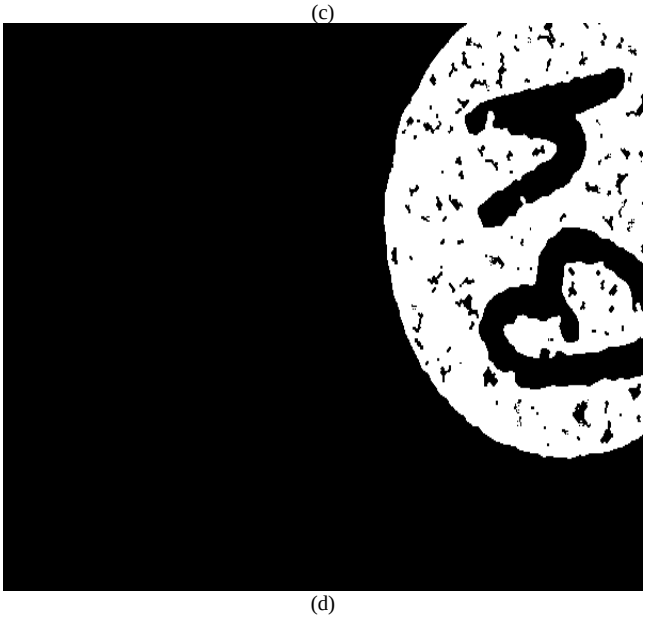

(d)

Fig. 2: (a) Original image with unremoved stickers. (b) Defect detection using Image Difference algorithm with auto-thresholding. (c) Defect detection using Image Difference algorithm with manual thresholding aimed to remove falsely detected pin through hole areas. (d) Proposed algorithm's defect detection.

For learning dataset, a total of 12 images which including 3 images with foreign material are used in learning process which described in **Algorithm 1**. **Fig. 3** is an example of good sample used in learning process. **Fig. 4** is a learnt sample with solder contamination which included in the learning dataset. However, the inclusion of defective images is shown experimentally do not affect the defect detection capability of proposed algorithm. Rather, it is detected as contaminated with foreign material as shown in **Fig. 5**. The generation of reference table for histogram distances marked the end of **Algorithm 1**.

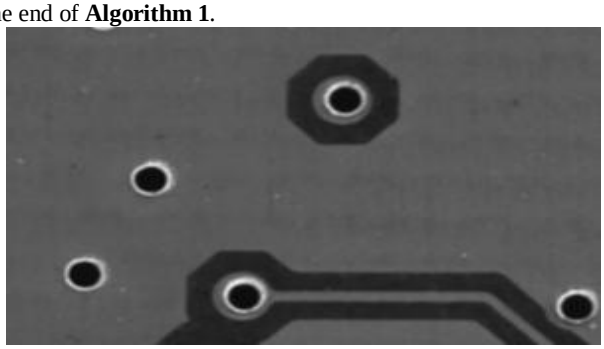

Fig. 3: Example of good sample for learning dataset.

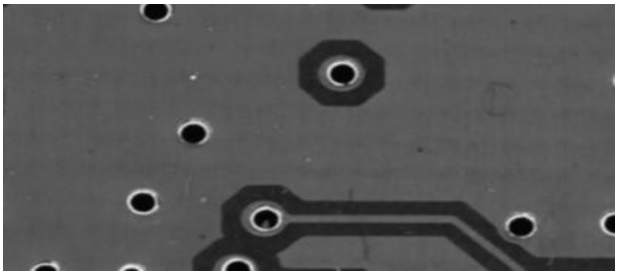

Fig. 4: Learning sample with solder contamination.



Fig. 5: Solder contamination from learning dataset caught as defect.

For validation, all 60 images are processed using proposed algorithm described in **Algorithm 2**. A surface defect heat map is generated. **Fig. 6** is an example of generated heat map using proposed algorithm. To highlight defects in all samples, hysteresis thresholding using threshold, $\tau = 40$ is done on resulted heat map. The result of the hysteresis thresholding is a binary map highlighting defective region. Using the same learning set and threshold, defect detection rate for 60 unpopulated location on a PCB is 100%. Foreign materials in 51 images are successfully marked as FAIL while remaining 9 images are marked as PASS. Five samples including 4 defective and 1 good is consolidated in **Fig. 7**.

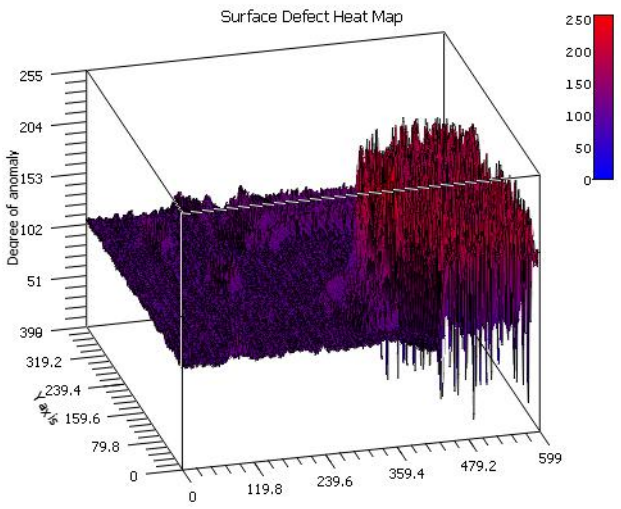

Fig. 6: Surface defect map heat map generated using Algorithm 2.

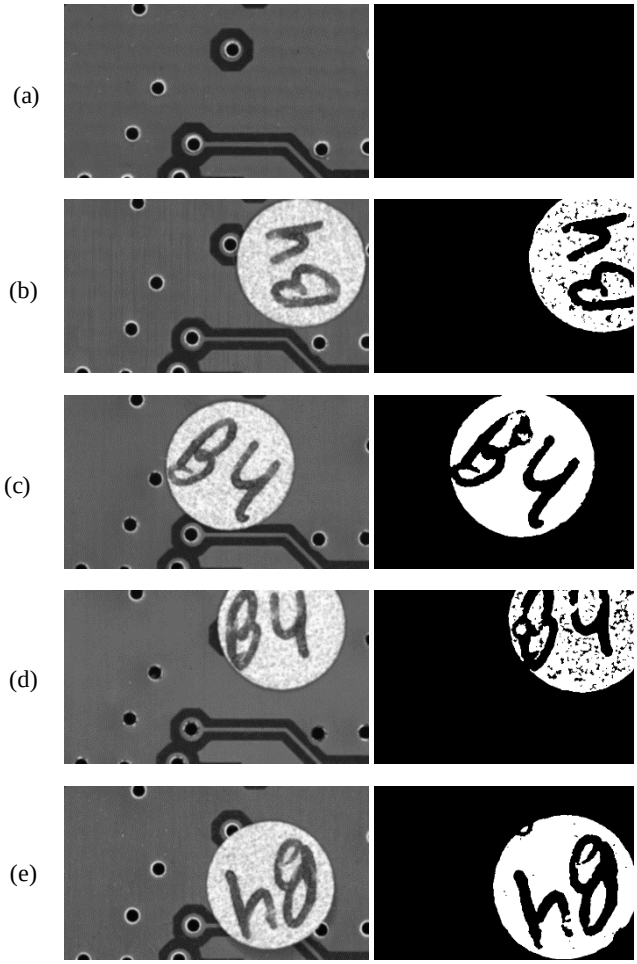

Fig. 7: Defect detection using proposed algorithm of 5 samples. Sample (a) is PASS unit and no defect is highlighted in the result. Sample (b), (c), (d) and (e) are FAIL units, contaminated with unremoved stickers.

Average learning and inspection time for each unit is 3.53s and 98ms respectively. It is suitable for real time inspection application. To examine further, learning and inspection time (per sample) for varying learning dataset size is studied. The overall trend is shown in the graphs shown in **Fig. 8** and **Fig. 9**. Due to the fundamental concept of the algorithm, both learning and inspection time does not depend on learning dataset size. It is different from non-golden template based multiple templates inspection algorithms where learning dataset size will affect inspection time. This is because suitable templates need to be selected during inspection. It has distinguished itself from neural-network algorithms where back-propagating learning process time grows as learning dataset size grows.

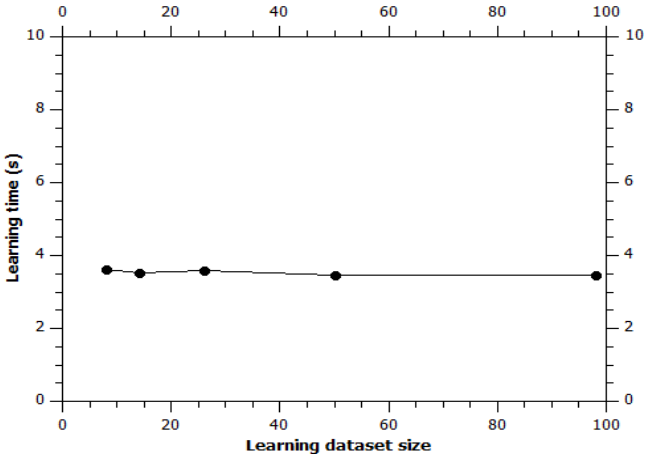

Fig. 8: Graph of total learning time against learning dataset size.

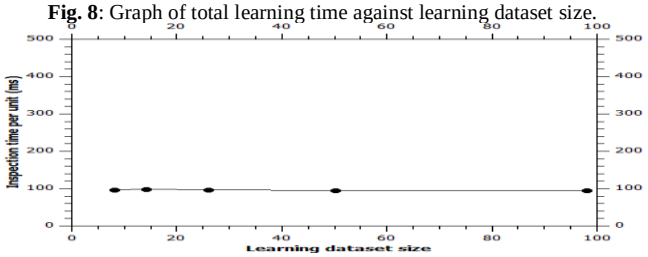

Fig. 9: Graph of average inspection time per sample against learning dataset size.

5. Conclusion

We propose a new surface defect detection strategy using histogram distance based multiple template anomalies detection algorithm. Proposed algorithm can handle slight lighting, texture, alignment and product variation. Experiment results using industrial samples demonstrate excellence defect detection capability, even with very simple image registration algorithm which is not alignment and rotation invariant. Proposed algorithm has real time and consistent learning and inspection time. Moreover, proposed algorithm's learning and inspection process is scalable to learning dataset size.

References

[1] D.-M. Tsai, M.-C. Chen, W.-C. Li, and W.-Y. Chiu, "A fast regularity measure for surface defect detection," *Mach. Vis. Appl.*, vol. 23, no. 5, pp. 869–886, Sep. 2012.

[2] X. Xie, "A review of recent advances in surface defect detection using texture analysis techniques," ... *Lett. Comput. Vis. Image Anal.*, vol. 7, no. 3, pp. 1–22, 2008.

[3] D. M. Tsai and J. Y. Luo, "Mean shift-based defect detection in multicrystalline solar wafer surfaces," *IEEE Trans. Ind. Informatics*, vol. 7, no. 1, pp. 125–135, 2011.

[4] S. Huang and Y.-C. Pan, "Automated visual inspection in the semiconductor industry: A survey," *Comput. Ind.*, vol. 66, pp. 1–10, 2015.

[5] M. Moganti, F. Ercal, C. H. Dagli, and S. Tsunekawa, "Automatic PCB Inspection Algorithms: A Survey," *Comput. Vis. Image Underst.*, vol. 63, no. 2, pp. 287–313, 1996.

[6] S. Son, "Reference-based Defect Detection on OLED Images using Local Gaussian Distribution," vol. 3, no. 3, pp. 19–34, 2015.

[7] S. Mei, H. Yang, and Z. Yin, "An Unsupervised-Learning-Based Approach for Automated Defect Inspection on Textured Surfaces," pp. 1–12, 2018.

[8] P. Xie and S. U. Guan, "Golden-template self-generating method for patterned wafer inspection," *Mach. Vis. Appl.*, vol. 12, no. 3, pp. 149–156, 2000.

[9] Z. Ibrahim and S. A. R. Al-attas, "Wavelet-Based Printed Circuit Board Inspection System," *Int. J. Signal Process.*, vol. 1, no. 2, pp.

73–79, 2005.
[10] D. M. Tsai, C. T. Lin, and J. F. Chen, "The evaluation of normalized cross correlations for defect detection," *Pattern Recognit. Lett.*, vol. 24, no. 15, pp. 2525–2535, 2003.
[11] D. M. Tsai and C. H. Yang, "A quantile-quantile plot based pattern matching for defect detection," *Pattern Recognit. Lett.*, vol. 26, no. 13, pp. 1948–1962, 2005.
[12] D. M. Tsai, I. Y. Chiang, and Y. H. Tsai, "A shift-tolerant dissimilarity measure for surface defect detection," *IEEE Trans. Ind. Informatics*, vol. 8, no. 1, pp. 128–137, 2012.
[13] V. H. Gaidhane, Y. V Hote, and V. Singh, "An efficient similarity measure approach for PCB surface defect detection," *Pattern Anal. Appl.*, 2017.
[14] H. Kong, J. Yang, and Z. Chen, "Accurate and Efficient Inspection of Speckle and Scratch Defects on Surfaces of Planar Products," *IEEE Trans. Ind. Informatics*, vol. 13, no. 4, pp. 1855–1865, 2017.
[15] R. Ren, T. Hung, and K. C. Tan, "A Generic Deep-Learning-Based Approach for Automated Surface Inspection," *IEEE Trans. Cybern.*, vol. 48, no. 3, pp. 929–940, 2018.
[16] K. Briechle and U. D. Hanebeck, "Template matching using fast normalized cross correlation," *Proc. SPIE*, vol. 4387, pp. 95–102, 2001.